Smart Structures and Systems, *Vol. 26, No. 4* (*2020*) *435-449*
DOI: https://doi.org/10.12989/sss.2020.26.4.435

Simultaneous out-of-plane and in-plane vibration mitigations of offshore monopile wind turbines by tuned mass dampers

Haoran Zuo, Kaiming Bi* and Hong Hao

Centre for Infrastructure Monitoring and Protection, School of Civil and Mechanical Engineering, Curtin University, Kent Street, Bentley, WA 6102, Australia

(*Received November 6 2019, Revised May 4 2020, Accepted July 27 2020*)

Abstract. To effectively extract the vast wind resource, offshore wind turbines are designed with large rotor and slender tower, which makes them vulnerable to external vibration sources such as wind and wave loads. Substantial research efforts have been devoted to mitigate the unwanted vibrations of offshore wind turbines to ensure their serviceability and safety in the normal working condition. However, most previous studies investigated the vibration control of wind turbines in one direction only, i.e., either the out-of-plane or in-plane direction. In reality, wind turbines inevitably vibrate in both directions when they are subjected to the external excitations. The studies on both the in-plane and out-of-plane vibration control of wind turbines are, however, scarce. In the present study, the NREL 5 MW wind turbine is taken as an example, a detailed three-dimensional (3D) Finite Element (FE) model of the wind turbine is developed in ABAQUS. To simultaneously control the in-plane and out-of-plane vibrations induced by the combined wind and wave loads, another carefully designed (i.e., tuned) spring and dashpot are added to the perpendicular direction of each Tuned Mass Damper (TMD) system that is used to control the vibrations of the tower and blades in one particular direction. With this simple modification, a bi-directional TMD system is formed and the vibrations in both the out-of-plane and in-plane directions are simultaneously suppressed. To examine the control effectiveness, the responses of the wind turbine without control, with separate TMD system and the proposed bi-directional TMD system are calculated and compared. Numerical results show that the bi-directional TMD system can simultaneously control the out-of-plane and in-plane vibrations of the wind turbine without changing too much of the conventional design of the control system. The bi-directional control system therefore could be a cost-effective solution to mitigate the bi-directional vibrations of offshore wind turbines.

Keywords: offshore wind turbine; vibration mitigation; TMD

1. Introduction

Offshore wind energy, as one of the renewable energies, experienced rapid development in the last decade and is becoming a main contributor to the new electricity generation. As reported by the Global Wind Energy Council (GWEC 2018), a historical record of 4,334 MW of new offshore wind power was installed worldwide in 2017, an 87% increase compared to that in 2016, and the cumulative offshore wind capacity in 2017 reached 18,814 MW. To maximize the wind energy extraction in marine areas, offshore wind turbines are erected with slender tower and large rotor. For example, the tower height and rotor diameter of the conceptual Haliade-X 12 MW offshore wind turbine are 150 m and 220 m, respectively (GWEC 2018). These high-rise and flexible structures are susceptible to external excitations such as wind and wave loads, and the excessive vibrations can compromise the wind energy output and decrease the fatigue life and may even lead to the catastrophic collapse of wind turbines in the harsh environmental conditions. It is imperative to mitigate the excessive vibrations of offshore wind turbines by using vibration control techniques to ensure their safety and serviceability and to lower the maintenance cost when they are in the normal parked and operating conditions.

Although structural control discipline has been well developed and various control devices and algorithms have been proposed to reduce the structural responses (e.g., Zhang *et al*. 2010, Zhang 2014, Zhang and Ou 2015, Zhang and Wang 2019, 2020), using control devices to mitigate the adverse vibrations induced by wind, wave and/or seismic loads of offshore wind turbines is a relatively new research field. A state-of-art review of the current vibration control techniques and their applications in wind turbines was provided by Zuo *et al*. (2020). These control techniques can be generally divided into passive, semi-active and active categories depending on whether external power is needed. Compared to the semi-active and active strategies, passive control methods need no power input and they have been widely applied to mitigate the vibrations of wind turbines especially the tower vibrations. For example, Tuned Mass Dampers (TMDs) were adopted by Murtagh *et al*. (2008), Lackner and Rotea (2011), Zhao *et al*. (2018) and Ghassempour *et al*. (2019), and Colwell and Basu (2009), Mensah and Dueñas-Osorio (2014) and Hemmati *et al*. (2019) proposed using Tuned Liquid Column Dampers

*Corresponding author, Senior Lecturer,
E-mail: kaiming.bi@curtin.edu.au

ISSN: 1738-1584 (Print), 1738-1991 (Online)

(TLCDs). Very recently, some new techniques have been developed to further improve the performance of conventional TMD systems. For example, it is well known that the control performance of TMD is dependent on the mass ratio between the control device and main structure, and larger mass ratio generally results in better and more robust control effectiveness. Hu *et al.* (2018) and Zhang *et al*. (2019) proposed inerter-based TMD systems to amplify the physical mass of TMD in order to increase the control effectiveness. Considering the limited space in the nacelle, Zuo *et al*. (2017) and Hussan *et al.* (2018) suggested installing multiple small TMDs (MTMDs) to mitigate the seismic responses of the tower. It was observed that, besides controlling the vibration associated with the fundamental vibration mode, MTMDs can effectively mitigate high-mode vibrations with improved robustness.

It should be noted that, in the previous studies, wind was assumed as the main driving force for the wave, and wind and wave loads were acting on the tower in the same direction, i.e., the out-of-plane direction of the wind turbine. Only the out-of-plane vibration of the tower was therefore controlled. However, recorded metocean data indicate that the directions of wind and wave are not necessarily always aligned (Stewart and Lackner 2014). The wind-wave misalignment could lead to the tower vibrates in both the in-plane and out-of-plane directions simultaneously. Moreover, the wind loads acting on the blades can result in the in-plane vibration of the tower since the wind loads on the blades have a component in the in-plane direction due to the twisted shape of the blades. The aerodynamic damping in the in-plane direction is normally very low, large tower responses thus might appear in this direction and need to be suppressed. In order to control the in-plane vibration of the tower, Zhang *et al*. (2016) used a Tuned Liquid Damper (TLD). Stewart and Lackner (2014) used two orthogonal TMDs to mitigate the in-plane and out-of-plane vibrations of the wind turbine tower induced by the wind-wave misalignment by using the publically available program FAST-SC. A three-dimensional (3D) pendulum damper was developed by Sun and Jahangiri (2018, 2019) and Sun *et al*. (2019) to control the tower vibrations, and the structural responses were estimated by using the home-made codes, in which the tower and each blade were simplified as two Degrees-Of-Freedom (DOFs) systems (one in the in-plane direction and another one in the out-of-plane direction), respectively. Zhao *et al*. (2018) installed two linear TMDs in the nacelle, and an experimental study was carried out to control the seimic-induced vibrations of the tower. The control effectiveness of these dampers in the in-plane and out-of-plane vibration mitigation was numerically (Stewart and Lackner 2014, Sun and Jahangiri 2018, 2019, Sun *et al*. 2019) or experimentally (Zhao *et al*. 2018) demonstrated. However, it should be noted that, only the tower vibrations were of interest, and the bi-directional vibration mitigation of the blades was not reported.

Compared to the wind turbine tower, the research works on the vibration mitigation of the blades are relatively scarce. Similarly, the vibrations of the blades occur in both the in-plane and out-of-plane directions and they are usually coupled with each other due to the twisted shape of the blades as mentioned above. However, this coupling effect was not considered in the previous studies, and the out-of-plane and in-plane vibrations of the blades were controlled separately. Arrigan *et al*. (2011) and Zuo *et al*. (2019) used semi-active TMDs and MTMDs respectively to control the out-of-plane vibrations of the blades, which highlighted the feasibility of using TMDs in supressing the vibrations of the blades. Zhang *et al*. (2014, 2015a, b) developed roller dampers TLCDs, TLDs and Basu *et al*. (2016) used Circular Liquid Column Dampers (CLCDs) to enhance the damping of the blades in the in-plane direction. In these studies, the mass of the control device was set very small by taking advantage of the centrifugal acceleration. These control methods are therefore more effective when the wind turbine is in the operating condition. In addition, active and semi-active control techniques have also been used to mitigate the in-plane vibrations of the blades (e.g., Staino *et al*. 2012, Fitzgerald *et al*. 2013, Arrigan *et al*. 2014, Fitzgerald and Basu 2014, Dinh *et al*. 2016). Although the effectiveness of these active and semi-active control strategies were numerically confirmed and reasonable structural response reductions were achieved, these control techniques need relatively complex control configurations and external power input, the practical application of these active control strategies might be an issue since the internal space of the blades is even smaller than that in the nacelle.

The critical literature reveals that most previous studies focused on the vibration control of wind turbines in one particular direction. When the vibration in one direction was of interest, the vibration in the other direction was not considered. In other words, the vibrations were controlled separately. Very few studies, to the best knowledge of the authors, only Stewart and Lackner (2014), Sun and Jahangiri (2018, 2019), Zhao *et al*. (2018) and Sun *et al*. (2019) considered the simultaneous control of the out-of-plane and in-plane vibrations of the tower though the coupling is inevitable, yet the bi-directional vibration mitigation of the blades was not addressed in Stewart and Lackner (2014), Sun and Jahangiri (2018, 2019), Zhao *et al*. (2018) and Sun *et al*. (2019).

This paper proposes using the bi-directional TMD system, a system that can be conveniently achieved by perpendicularly adding another properly designed (i.e., tuned) spring and dashpot to each of the TMD system that is used to control the vibration of the wind turbine in one particular direction to simultaneously control the out-of-plane and in-plane vibrations of both the tower and blades of offshore wind turbines. The NREL 5 MW wind turbine is taken as an example, and a detailed 3D Finite Element (FE) model is developed in the commercially available FE code ABAQUS. The tower and blades are explicitly modelled. The combined wind and wave loads are considered as external vibration sources, and the responses of the parked and operating wind turbines without control, with separate control device and the proposed bi-directional control system are calculated and systematically compared. The structure of this paper is organized as follows: the detailed information of the FE model is given in Section 2; Section 3 briefly introduces the simulation methods of wind and wave loads; the parameters of the TMD system are calculated in

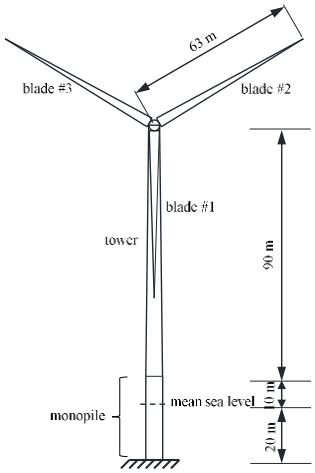

(a) NREL 5 MW wind turbine

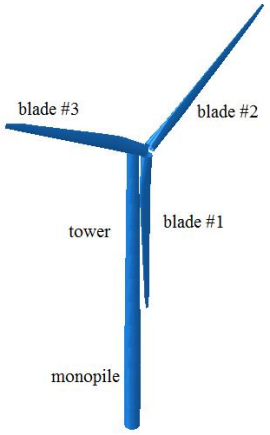

(b) FE model

Fig. 1 Offshore wind turbine model

Table 1 Properties of the NREL 5 MW wind turbine

Blade	Rotor diameter	126 m
	Hub height	90 m
	Cut-in, rated and cut-out wind speed	3 m/s, 11.4 m/s, 25 m/s
	Cut-in and rated rotor speed	6.9 rpm, 12.1 rpm
	Length	61.5 m
	Overall (integrated) mass	17,740 kg
	Structural damping ratio	0.5%
Hub and nacelle	Hub diameter	3 m
	Hub mass	56,780 kg
	Nacelle mass	240,000kg
Tower	Height above water	87.6 m
	Bottom and top outer diameters	6 m, 3.87 m
	Bottom and top wall thicknesses	0.027 m, 0.019 m
	Overall (integrated) mass	347,460 kg
	Structural damping ratio	1%
Monopile	Total length	30 m
	Outer diameter	6 m
	Wall thickness	0.060 m

Table 2 Material properties of steel and polyester

Component	Material	Density (kg/m^3)	Young's modulus (GPa)	Poisson's ratio	Yield strength (MPa)	Plastic strain
Blade	Polyester	1850	38	0.3	700	0.02
Tower	Steel	8500	210	0.3	235	0.01
Monopile above water	Steel	7850	210	0.3	235	0.01
Monopile in water	Steel	8880	210	0.3	235	0.01

Section 4; Section 5 discusses the dynamic responses of the wind turbine without and with different control strategies, and some concluding remarks are given in Section 6.

2. FE model

The NREL 5 MW wind turbine is chosen as an example in the present study since its geometrical configurations were given in detail in Jonkman *et al*. (2009). Fig. 1(a) shows the main dimensions of the wind turbine, and the detailed information are tabulated in Table 1. It should be noted that, except the thickness, all other information of the blades can be found in Jonkman *et al*. (2009). In the present study, a uniform thickness is assumed and the mass of the blades is ensured to be the same as that in Jonkman *et al*. (2009). With this assumption, the thickness of the blades is computed as 0.019 m (Zuo *et al*. 2018).

In most previous studies on dynamic response analyses and/or vibration control of wind turbines, normally only the tower was modelled by ignoring the blades (e.g., Colwell and Basu 2009) or the blades were considered by simplifying as a two DOFs system (e.g., Fitzgerald and Basu 2014, Sun and Jahangiri 2018, 2019). To some extent, this practice is reasonable when the wind turbine is in the parked condition. However, when the wind turbine is in the operating condition, the centrifugal acceleration can be generated by the rotation of the blades, which can alter the vibration characteristics and further influence the overall responses of the wind turbine. Moreover, the interaction between the tower and blades is inevitable, and the wind loads along the length of the blades are different. To more realistically capture the structural responses of the wind turbine, the real geometrical configurations of the blades are considered and the rotation of the blades is modelled in the present study. The detailed information of the FE model was given in one of the authors' previous studies (Zuo *et al*. 2018), which is not introduced here for conciseness, and only the sketch of the FE model is shown in Fig. 1(b).

Table 2 tabulates the material properties of the blades, tower and monopile. For the monopile in the sea water, the vibrating monopile can impart an acceleration to the surrounding sea water, which in turn causes inertial force to the monopile. This interaction between the monopile and sea water is considered by using the added mass method in the present study, and interested readers can refer to DNV

Table 3 Fundamental vibration frequencies and modes of the wind turbine (parked condition)

Mode description	Frequency (rad/s)
1st tower in-plane	1.514
1st tower out-of-plane	1.516
1st blade out-of-plane	3.763
1st blade in-plane	7.774

(2010) and Zuo *et al*. (2018) for more detailed calculation of the added mass.

The damping of an offshore wind turbine consists of structural, aerodynamic and hydrodynamic damping, which account for the contributions of the structure itself, wind and surrounding sea water respectively. The detailed values of these damping components have been introduced in Zuo *et al*. (2018, 2019), which are not presented herein. Add all the components together, the damping ratio of the tower is 1.23%. The value is 4% in the out-of-plane direction for the rotating blades; for the parked blades or in the in-plane direction, it is 0.5%.

After the FE model is developed, an eigenvalue analysis is carried out to calculate the vibration frequencies and mode shapes of the wind turbine. It should be noted that, in the modal analysis, the rotation of the blades cannot be explicitly considered by using ABAQUS, and only the parked condition is considered when these vibration characteristics (vibration frequencies and modes) are calculated. Since the energies of wind and wave loads considered in the present study concentrate in the low frequency range, normally only the fundamental vibration modes of the tower and blades can be excited, the fundamental modes are thus mitigated in the present study. Table 3 tabulates the first vibration frequencies and the corresponding vibration modes of the tower and blades in the in-plane and out-of-plane directions.

3. Wind and wave loads

In the present study, the wind turbine is subjected to the combined wind and wave loads, which are constantly experienced by offshore wind turbines during their lifetimes. The wind and wave loads are stochastically simulated based on the sophisticated simulation techniques and are briefly introduced in this section for completeness. Detailed information regarding the wind and wave simulations can be found in Zuo *et al*. (2018).

The wind loads at different locations along the tower are different, however, as the height of the tower is around 90 m in the present study, the wind load in every 10 m is assumed to be the same for simplicity, nine segments are therefore adopted in the wind load simulation. The wind speed in each segment is modelled by the Kaimal spectrum (Murtagh *et al*. 2005). Moreover, the similarity of the wind loads between different segments is described by a spatial coherency loss function in the present study (Huang *et al*. 2013).

As tabulated in Table 1, the maximum energy output of

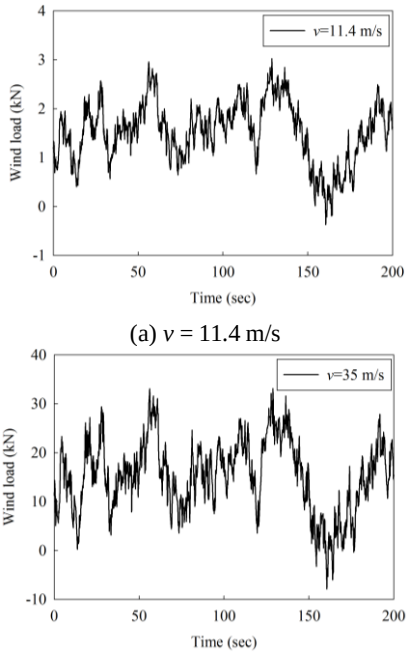

(a) v = 11.4 m/s

(b) v = 35 m/s

Fig. 2 Wind loads at the tower top when the wind turbine is in the (a) operating and (b) parked conditions

wind turbine will be achieved when the mean wind speed at the hub height is 11.4 m/s, and the wind turbine stops rotating when the wind speed is above 25 m/s in order to protect the electrical and mechanical components. In the present study, two operational conditions (i.e., the operating and parked conditions) are considered, and the mean wind speed of 11.4 m/s and 35 m/s is used in each condition. Fig. 2 shows the wind loads at the top segment when the NREL 5 MW wind turbine is in the operating and parked conditions respectively. The wind loads in the other segments are not presented for conciseness.

To estimate the wind loads on the blades, the Blade Element Momentum (BEM) method (Hansen 2008) is adopted in the present study. Fig. 3(a) shows the in-plane and out-of-plane wind loads on the three blades when the wind turbine rotates at a rated velocity of 12.1 rpm, and the corresponding wind loads for the parked condition (in which the mean wind speed is 35 m/s) are shown in Fig. 3(b). As shown in Fig. 1, the locations of the blades #2 and #3 are symmetric when the wind turbine is in the parked condition, the wind loads on these two blades are therefore the same. Only the wind loads on blade #2 are presented in Fig. 3(b) for conciseness.

As shown in Fig. 1, part of the monopile is in the sea water, the wave load acting on the monopile is considered, and the JONSWAP spectrum (Hasselmann *et al*. 1973) is used to simulate the sea surface elevation. Then the wave load is calculated by the Morison formula. Similar to the wind loads on the tower, the wave loads along the height of the monopile are different. For the sake of simplicity, the monopile in the sea water is equally divided into two segments and the wave load in each segment is assumed the same. Fig. 4 shows the wave loads at the mean sea level

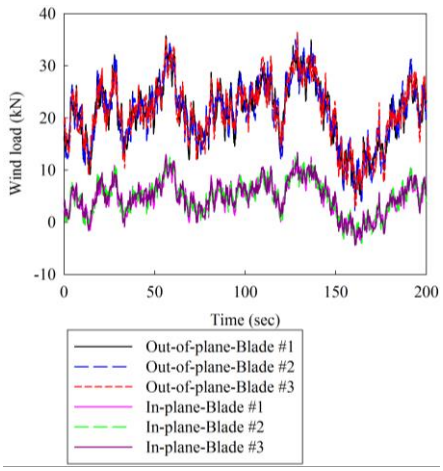

(a) Operating condition

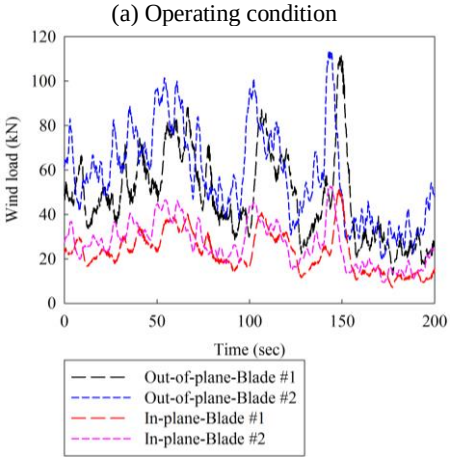

(b) Parked condition

Fig. 3 Wind loads on the blades under different operational conditions

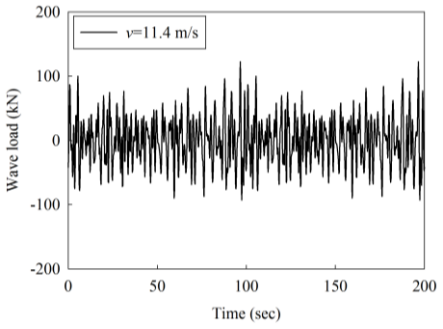

(a) v = 11.4 m/s

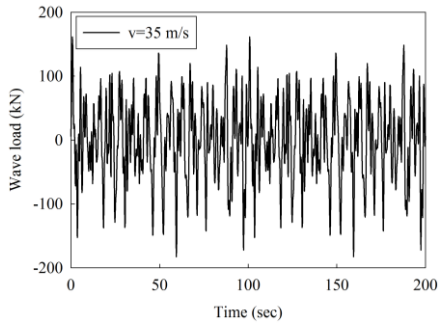

(b) v = 35 m/s

Fig. 4 Wave loads at the mean sea level

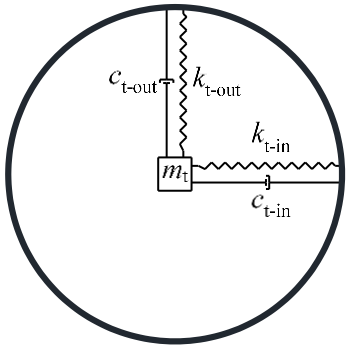

Fig. 5 Main structure-bi-directional TMD system

when the mean wind speeds at the hub height are 11.4 m/s and 35 m/s, respectively.

In the wind and wave load simulations, the blades, tower and monopile are divided into a few segments as mentioned above. In the FE model, a reference point is developed in each segment and coupled with the cross section of the corresponding segment, the simulated wind and wave loads are applied to these reference points as the external vibration sources. The wave loads on the monopile and wind loads on the tower are applied in the fore-aft (out-of-plane) direction of the tower, and the wind loads on the blades are applied in the in-plane and out-of-plane directions, respectively.

4. Bi-directional TMD system and parameters

As discussed above, the vibrations of the tower and blades of offshore wind turbines were normally considered separately, and a TMD system was generally used to control the vibration in one direction. For example, if the vibration in the out-of-plane direction is of interest, the spring and dashpot will be installed in the out-of-plane direction. Literature review also indicates that the out-of-plane and in-plane vibrations of offshore wind turbine are inevitably coupled with each other, and the vibrations in both directions may significantly influence the performance of the wind turbines, thus they should be controlled simultaneously. In the present study, instead of installing spring and dashpot in one direction, another properly designed spring and dashpot are installed in the perpendicular direction of the original TMD system to form a bi-directional TMD system as shown in Fig. 5. By doing so, the vibrations in both directions can be controlled simultaneously as will be demonstrated in the numerical results. It should be noted that, compared to the conventional uniaxial TMD system, only another spring and dashpot need to be added, which will not change too much of the conventional design. The bi-directional control system therefore could be a cost-effective solution to mitigate the bi-directional vibrations of offshore wind turbines.

Fig. 5 shows the sketch of the bi-directional TMD system, in which the auxiliary mass (m_t) is attached to the vibrating main structure (i.e., tower and blade) by two perpendicular springs ($k_{t\text{-}in}$ and $k_{t\text{-}out}$) and dashpots ($c_{t\text{-}in}$ and

$c_{t\text{-out}}$). As demonstrated in many previous studies, the springs and dashpots should be carefully selected in order to make the system effective, and this is normally dubbed tune. In the present study, the displacement responses of the tower and blades are of interest, and the numerical searching technique is then used to obtain the corresponding optimal values by minimizing the mean square displacements of the tower and blades under an assumed mass ratio, which is briefly introduced in this section.

To optimize the TMD systems, two parameters are defined

$$\gamma = \frac{\omega_t}{\omega_s} \tag{1}$$

$$\mu = \frac{m_t}{m_s} \tag{2}$$

in which γ and μ are the frequency (ω) and mass (m) ratios of the TMD to the main structure, respectively, with the subscripts *t* and *s* denoting the TMD and the main structure. The stiffness (k_t) and damping coefficient (c_t) of the TMD then can be estimated as

$$k_t = m_t\omega_t^2 = \mu m_s\gamma^2\omega_s^2 \tag{3}$$

$$c_t = 2\zeta_t m_t\omega_t = 2\zeta_t\mu m_s\gamma\omega_s \tag{4}$$

where ζ_t is the damping ratio of the TMD.

As discussed above, the displacements of the tower and blades in the in-plane and out-of-plane directions are aimed to be controlled. The mean square displacement of the wind turbine in a particular direction can be expressed as

$$\sigma^2 = \int_{-\infty}^{+\infty} |H_s(\omega)|^2 S(\omega) d\omega \tag{5}$$

in which

$$H_s(\omega) = [\omega_s^2 - 2i\omega\omega_s\zeta_s - \omega^2 - i\omega m_s^{-1} Z(\omega)]^{-1} \tag{6}$$

$$Z(\omega) = -i\omega \frac{m_t(\omega_t^2 - 2i\omega\omega_t\zeta_t)}{\omega_t^2 - 2i\omega\omega_t\zeta_t - \omega^2} \tag{7}$$

where ζ_s is the damping ratio of the main structure as given in Section 2.

Substituting Eqs. (6) and (7) into Eq. (5), the optimal frequency ratio γ and damping ratio ζ_t can be obtained via the numerical searching technique by minimizing the mean square displacement of the main structure under a given mass ratio μ.

It should be noted that the vibration characteristics (frequency ω_s and damping ratio ζ_s) of the tower and blades in the in-plane and out-of-plane directions are different as indicated in Section 2, the stiffness and damping coefficients in these two directions are optimized separately considering the different frequencies ($\omega_{s\text{-in}}$ and $\omega_{s\text{-out}}$) and damping ratios ($\zeta_{s\text{-in}}$ and $\zeta_{s\text{-out}}$) in the corresponding direction. Moreover, the vibration frequencies of the parked and rotating blades are also slightly different (Zuo *et al.* 2018, 2019) due to the centrifugal stiffness generated by rotation. In practice, however, it is not feasible to change the parameters of the control devices during its service life. In the present study, the vibration frequencies of the parked condition (i.e., Table 3) are used to estimate the parameters of the bi-directional TMD systems in both the parked and operating conditions. Table 4 tabulates the optimal values of the TMD systems in different directions by assuming a mass ratio of 3%.

Table 4 Optimal stiffness and damping coefficients of the bi-directional TMD systems

Component		γ	ζ_t	m_t (kg)	k_t (kN/m)	c_t (kNs/m)
Tower	In-plane	0.98	0.09	10424	23.63	2.83
	Out-of-plane	0.98	0.09		23.02	2.79
Blade	In-plane	0.97	0.09	532	30.25	0.72
	Out-of-plane	0.97	0.09		7.09	0.35

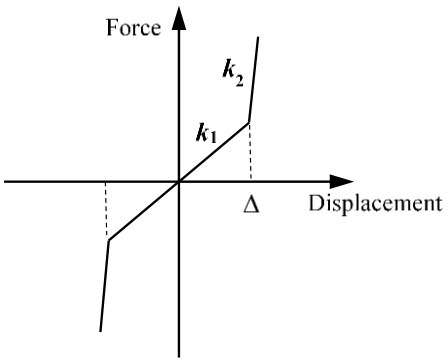

Fig. 6 Nonlinear force-displacement relationship of the spring element

The bi-directional TMD as shown in Fig. 5 are modelled by the mass, spring and dashpot elements in ABAQUS. However, it should be noted that the space in the tower and blades is limited, and the TMDs might penetrate the tower and blades in the numerical simulations, which is obviously not realistic, therefore the deformations of TMDs should be restrained in the numerical simulations. To avoid this unreasonable phenomenon, a nonlinear force-displacement relationship as shown in Fig. 6 is defined for the spring elements in the tower and blades, in which Δ is the allowable displacement. When the relative displacement between the TMDs and the tower/blade is smaller than Δ, the stiffness equals to the optimal value in Table 4, i.e., $k_1 = k_t$. If the relative displacement is larger than Δ, the spring becomes hard to be compressed and a stiffness k_2 is defined. $k_2 = 1\times10^6$ N/m is found to have a good balance between the effectiveness and efficiency (Zuo *et al.* 2019), and this value is adopted in the simulations.

It should be noted that the total movement of the additional mass is dependent on the deformations of the springs in the in-plane and out-of-plane directions. However, the interaction between the in-plane and out-of-plane directions is not considered in the optimization as adopted in some other researches (e.g., Zhao *et al.* 2018),

and the stiffness and dashpot coefficient in each direction are optimized independently.

5. Results and discussions

To examine the effectiveness of the proposed simultaneous control method, two operational scenarios are considered in the present study. In the first scenario, the wind turbine is in the parked condition with the mean wind speed of 35 m/s at the hub height. In the second scenario, the wind turbine is in the operating condition with the blades rotating at a uniform velocity of 1.27 rad/s, which corresponds to the rated rotor speed of the NREL 5 MW wind turbine (12.1 rpm) as tabulated in Table 1, and the mean wind speed is taken as 11.4 m/s. To mitigate the in-plane and out-of-plane vibrations of the tower, the bi-directional TMD system is installed at the tower top, where the allowable displacement in both directions is 1.916 m. The TMD system installed at the tower top is because, as mentioned in Section 2, only the fundamental vibration mode of the tower is normally excited by the wind and wave loads, in which the maximum displacement occurs at the tower top. The most effective control can be achieved by placing the TMD at the location with the maximum displacement. For the blades, similar to the tower, the maximum displacements appear at the corresponding tips. It is however not practical to install the TMD at the blade tip since the space at the tip is very limited. In the present study, a bi-directional TMD system is installed in each blade at the location with a distance of $L/6$ from the tip of the blade (where L is the length of the blade, i.e., L = 61.5 m). At this location, the allowable displacements of the TMD in the out-of-plane and in-plane directions are 0.324 m and 1.259 m, respectively. For comparison, the responses of the wind turbine without any control device and with separate TMD are also calculated. In particular, in the case of separate TMD, a single TMD is installed in either the out-of-plane or in-plane direction of the tower and blades to control the vibration in the corresponding direction.

To more straightforwardly show the control effectiveness, the following reduction ratio is defined

$$R = \frac{sd_1 - sd_2}{sd_1} \times 100\% \tag{8}$$

where sd_1 and sd_2 are the standard deviations of the in-plane and out-of-plane responses of the wind turbine without and with different control devices, respectively. It is obvious that the displacement responses along the height of the tower and the length of the blades are different and the largest responses occur at the top of the tower and the tip of the blades under the combined wind and wave loads as discussed. For conciseness, only the largest responses are examined to demonstrate the control effectiveness in the present study.

5.1 Parked condition

In this section, the wind turbine is assumed in the parked condition. In the numerical simulations, the external loads are applied to the wind turbine at t = 0 s. Owing to the dynamic effect onto the structure, the responses in the initial stage are not stable (Clough and Penzien 2003). The results in the first 10 s are therefore not analysed in this section, namely the discussions are based on the structural responses in the time period of 10-200 s during the stable response phase, not the initial transient response phase to better demonstrate the vibration control effectiveness.

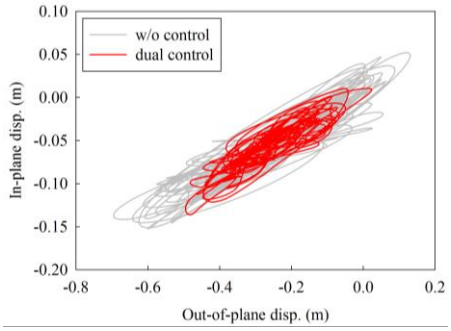

Fig. 7 Influence of bi-directional TMD system on the tower displacements under the parked condition

Fig. 7 shows the bi-directional motions at the top of the tower without and with the bi-directional TMD system when the wind turbine is in the parked condition. It can be seen that when the bi-directional TMD system is installed, the vibrations of the tower in the both directions are obviously reduced, which demonstrates the effectiveness of the proposed method. It should be noted that only the results of the cases with and without the bi-directional TMD system are shown in Fig. 7, the trajectories of the tower with the uniaxial TMD (i.e., the case of separate control) are not presented in the figure since when this case is considered, another two curves should be added to the figure, which makes the figure very difficult to read. The control effectiveness is presented and discussed in more detail by comparing the results in the out-of-plane and in-plane directions separately.

Fig. 8 shows the displacement time histories at the top of the tower in the in-plane and out-of-plane directions without and with different control methods. To straightforwardly compare the overall control effectiveness, the standard deviations of the in-plane and out-of-plane displacements at the top of the tower and the corresponding reduction ratios are summarized in Table 5. As shown, for the wind turbine without any control device, the standard deviations of the in-plane and out-of-plane displacements are 0.0440 m and 0.1790 m respectively. When the bi-directional TMD system is installed to simultaneously mitigate the in-plane and out-of-plane vibrations, these values become 0.0276 m and 0.1074 m and the reduction ratios are 37.3% and 40.0% respectively. When the vibrations are controlled by the separate TMD, the standard deviations are 0.0274 m and 0.1038 m and the reduction ratios are 37.7% and 42.0% respectively. It can be seen that the control effectiveness of the bi-directional TMD system is slightly less than that of the uniaxial TMD system. This is because, in the bi-directional vibration control system, the displacement of the TMD in one direction (e.g., the out-of-plane direction) is influenced by the spring and dashpot in

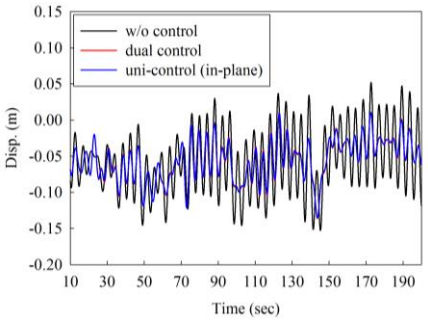

(a) In-plane

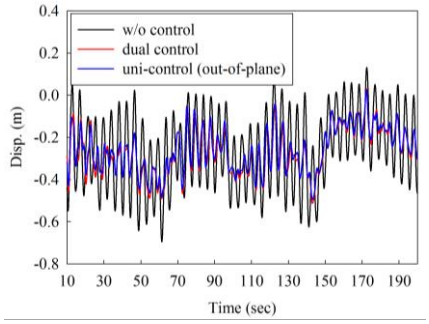

(b) Out-of-plane

Fig. 8 In-plane and out-of-plane displacements at the tower top under the parked condition

Table 5 Standard deviations of the in-plane and out-of-plane displacements and the corresponding reduction ratios under the parked condition

Direction	Location	W/o control	Dual control		Uni-control	
		sd (m)	*sd* (m)	*R*	*sd* (m)	*R*
In-plane	Tower top	0.0440	0.0276	37.3%	0.0274	37.7%
	Tip of blade #1	0.0649	0.0566	12.8%	0.0563	13.6%
	Tip of blade #2 (#3)	0.0788	0.0699	11.3%	0.0697	11.5%
Out-of-plane	Tower top	0.1790	0.1074	40.0%	0.1038	42.0%
	Tip of blade #1	0.6887	0.5502	20.1%	0.5159	25.1%
	Tip of blade #2 (#3)	0.6542	0.5855	10.5%	0.5736	12.3%

the other direction (the in-plane direction), such that the axes of these two springs are no longer perpendicular as shown in Fig. 9. The stiffness and damping components of the TMD in the in-plane and out-of-plane directions of the tower are therefore slightly different from the optimal values, and the control effectiveness are thus marginally decreased. However, it should be noted that, in the separate control case, only the vibration in one particular direction can be controlled. For the proposed method, the vibrations in both the in-plane and out-of-plane directions are mitigated simultaneously, and more importantly, the control effectiveness does not decrease too much compared to the uniaxial control system, which demonstrates the advantage

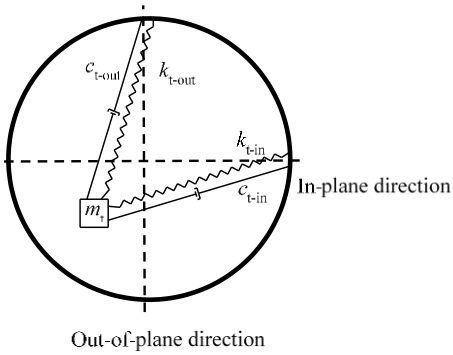

Fig. 9 Deformations of bi-directional TMD system

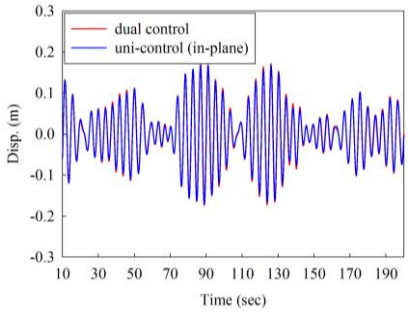

(a) In-plane TMD

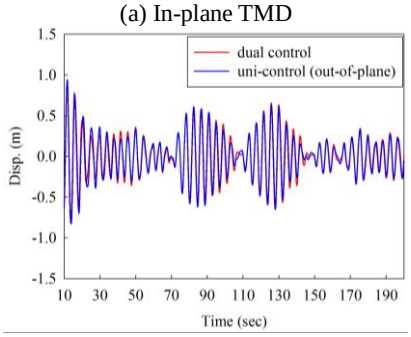

(b) Out-of-plane TMD

Fig. 10 Displacements of the in-plane and out-of-plane TMDs in the tower under the parked condition

of the proposed method.

As mentioned in Section 4, the spare space in the nacelle and blades is very limited, and the restrained space may influence the control effectiveness of the TMD or even result in the collision between the TMD and nacelle. The TMD stroke is thus an important issue in the vibration control of wind turbines and therefore investigated in the present study. Fig. 10 shows the displacement time histories of the in-plane and out-of-plane TMDs at the tower top in the bi-directional and uniaxial control systems when the wind turbine is in the parked condition. As shown, the displacements of the out-of-plane TMD are larger than those of the in-plane TMD since the tower vibrates dramatically in the out-of-plane direction as shown in Fig. 8(b), which leads to larger displacements of the out-of-plane TMD. Moreover, the maximum displacements of the TMDs in the uniaxial and bi-directional control systems are less than the radius of the cross section at the top of the tower (1.916 m), which means that the TMDs in both

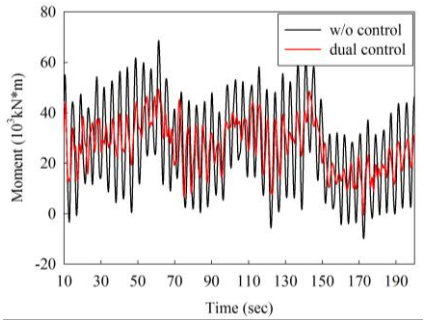

(a) In-plane

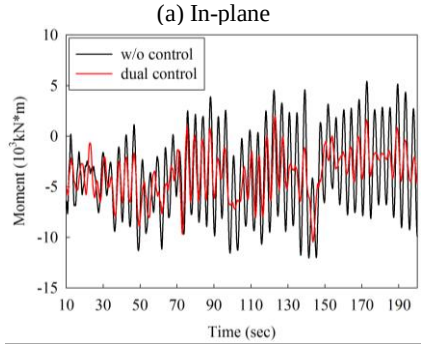

(b) Out-of-plane

Fig. 11 In-plane and out-of-plane bending moments at the tower bottom under the parked condition

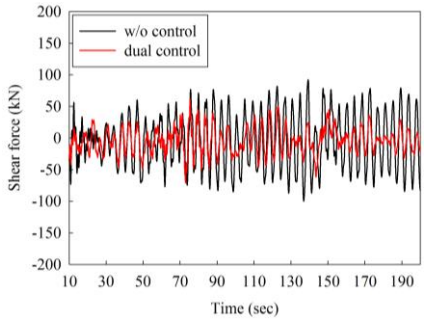

(a) In-plane

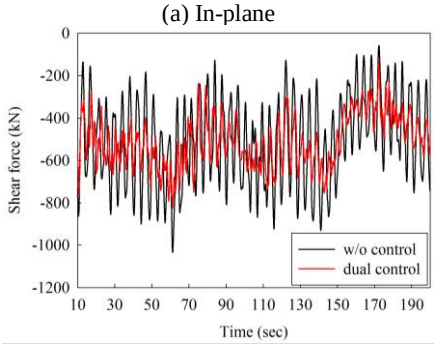

(b) Out-of-plane

Fig. 12 In-plane and out-of-plane shear forces at the tower bottom under the parked condition

control systems do not touch the tower. In addition, it can be seen that the displacements of the TMDs in the uniaxial control system are marginally smaller than those in the bi-directional control system though the control effectiveness of the uniaxial control system is more evident as discussed above. This is because, as illustrated in Fig. 9, the bi-directional TMD moves in both the in-plane and out-of-plane directions, and the deformations of the TMD neither aligned with the in-plane nor out-of-plane direction of the tower. For the uniaxial control system, the TMD only moves in the in-plane or out-of-plane direction. However, the in-plane and out-of-plane displacement components of the bi-directional TMD cannot be directly extracted from ABAQUS, only the resultant deformations of the in-plane and out-of-plane springs in the bi-directional TMD are compared in Fig. 10.

Table 6 Standard deviations of the in-plane and out-of-plane bending moments and shear forces at the tower base and the corresponding reduction ratios under the parked condition

Internal forces	Direction	W/o control	Dual control	
		sd	*sd*	*R*
Bending moment	In-plane	16830 kN·m	9786 kN·m	41.9%
	Out-of-plane	3909 kN·m	2235 kN·m	42.8%
Shear force	In-plane	43 kN	20 kN	53.5 %
	Out-of-plane	202 kN	121 kN	40.1%

Due to the high-rise and thin-walled geometrical characteristics of the wind turbine tower, it is vulnerable to fatigue damage or buckling under cyclic loads (e.g., wind and wave), and these calculations are related to the internal forces developed in the wind turbine, they are thus also discussed herein though the investigation on the fatigue damage or buckling is out of the scope of the present study.

The tower can be assumed as a cantilever beam, and it is obvious that the maximum internal forces appear at the bottom of the tower. Figs. 11 and 12 show the in-plane and out-of-plane bending moments and shear forces at this location without and with the bi-directional TMD system, respectively, and Table 6 summarizes the standard deviations in different cases and the corresponding reduction ratios. For the uniaxial TMD systems, since similar displacement control effectiveness is observed compared to the bi-directional control system as discussed above, the control effectiveness for the internal forces of these two systems should be similar as well. To more clearly show the curves, the results from the uniaxial control system are not presented. It can be seen that the bi-directional TMD system can obviously mitigate the internal forces developed in the tower. As shown in Table 6, the reduction ratios for the shear forces and bending moments in the in-plane and out-of-plane directions vary from about 40% to 54%. This obvious reduction can significantly increase the fatigue life (Sun and Jahangiri 2019) and buckling capacity (DNV 2002) of the wind turbine.

As for the blade responses, Fig. 13 shows the bi-directional motions at the tips of the three blades without and with the bi-directional TMDs when the wind turbine is in the parked condition. Figs. 14 and 15 respectively show the displacement time histories at the tips of the three blades in the in-plane and out-of-plane directions without and with different control systems. In the parked condition, the displacement responses of blade #3 are the same as those of blade #2 because the locations of blades #2 and #3 are

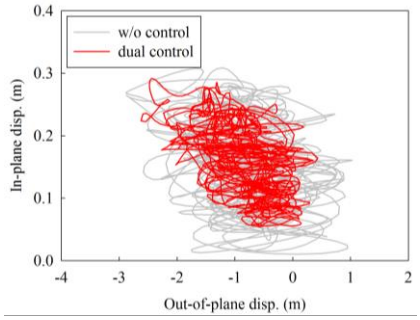

(a) Blade #1

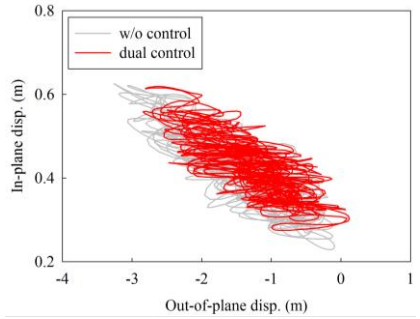

(b) Blade #2 (#3)

Fig. 13 Influence of bi-directional TMD system on the blade displacements under the parked condition

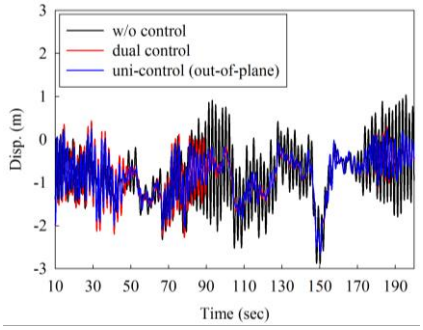

(a) Blade #1

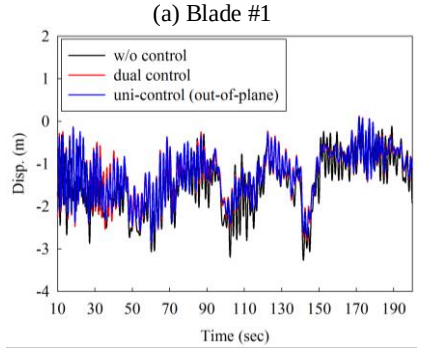

(b) Blade #2 (#3)

Fig. 15 Out-of-plane displacements at the blade tips under the parked condition

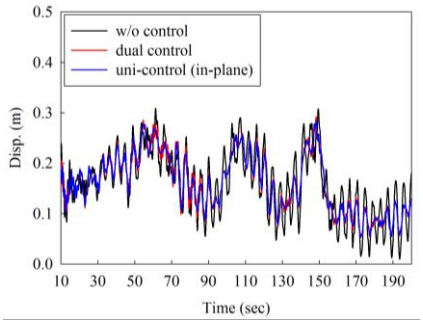

(a) Blade #1

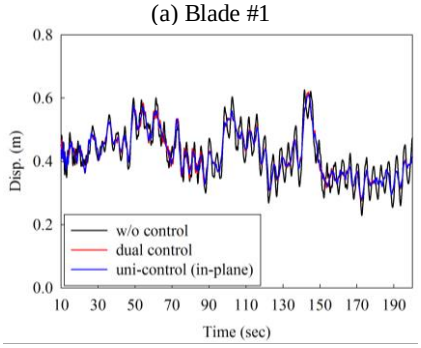

(b) Blade #2 (#3)

Fig. 14 In-plane displacements at the blade tips under the parked condition

symmetrical and the same wind loads are applied to these two blades as mentioned in Section 3. The standard deviations of the in-plane and out-of-plane displacements at the tips of the three blades and the corresponding reduction ratios are also tabulated in Table 5. Again, similar to the tower, using the bi-directional TMD system slightly decreases the control effectiveness compared to the uniaxial TMD system due to the reason explained above. For the in-plane vibrations, it can be seen from Table 5 that the TMD has the similar control effectiveness on blades #1 and #2. For the out-of-plane vibrations, the control effectiveness is, however, more evident for blade #1 compared to blade #2 for both control systems. The reason is that the wind loads on blade #2 are larger than those on blade #1, which result in larger displacement responses of blade #2 (see Fig. 15). In this case, larger relative displacements of the TMD in the blade are needed to dissipate more energy, however, the blade cannot provide enough space to allow the TMD to deform, which weakens the control performance.

Figs. 16 and 17 show the relative displacements of the in-plane and out-of-plane TMDs in blades #1 and #2, respectively. To clearly show the results, only the displacements of the TMDs in the time period of 100-200 s are presented. It can be seen that in the in-plane direction, both the TMDs in blades #1 and #2 can vibrate freely in the blades, while in the out-of-plane direction, the vibration for both TMDs are restrained by the limited space, and the relative displacements of the TMDs reach the allowable displacement (the red dashed lines in Fig. 17). As shown, the restraints for blade #2 are more evident compared to blade #1, which means that the function of the TMD in blade #2 is less developed, leading to the control effectiveness of the TMD in blade #2 less evident. It should be noted that in Fig. 16 the displacements of the in-plane TMDs in the uniaxial control system are smaller than those in the bi-directional control system, but the effectiveness of the uniaxial control system is more evident. This is because the figure shows the total deformations of the springs of the damper but not the component in the in-plane direction as

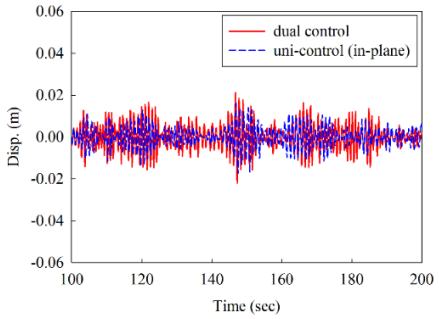

(a) Blade #1

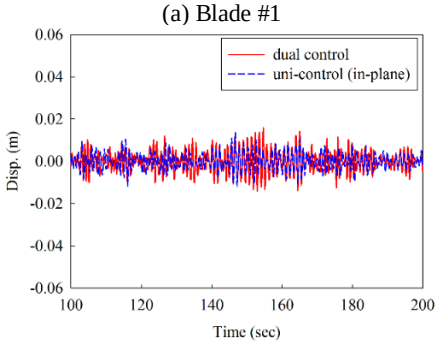

(b) Blade #2

Fig. 16 Displacements of the in-plane TMDs in blades #1 and #2 under the parked condition

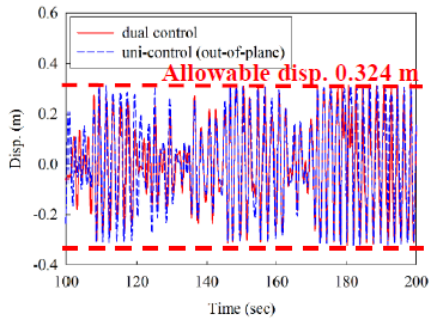

(a) Blade #1

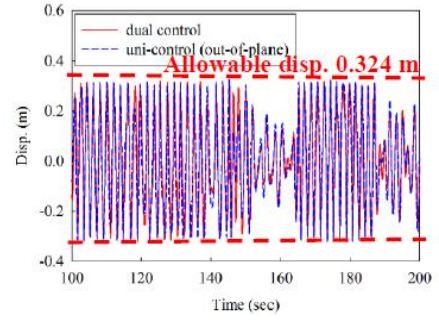

(b) Blade #2

Fig. 17 Displacements of the out-of-plane TMDs in blades #1 and #2 under the parked condition

discussed above. The displacement components of the bi-directional TMDs in the in-plane and out-of-plane directions are smaller than the corresponding displacement of the uniaxial TMDs.

The results in Table 5 also show that the control effectiveness for the blades is less than that for the tower.

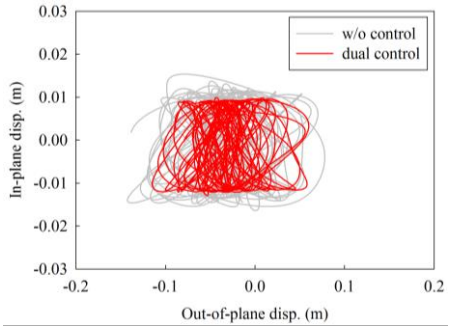

Fig. 18 Influence of bi-directional TMD system on the tower displacements under the operating condition

This is because, as discussed above, the TMD should install at the location with the maximum displacement to obtain the most effective control. In the tower, the TMD is installed at the tower top, while the TMD in each blade is installed at the location with a distance of $L/6$ from the tip of the blade, which impairs the control effectiveness for the blades.

5.2 Operating condition

In this section, the responses and control effectiveness of different control systems are compared and discussed when the wind turbine is in the operating condition. Similar to the application of external loads to the parked wind turbine, the response of the wind turbine system is unstable in the initial transient phase when the load is first applied (Zuo *et al*. 2018). To remove the influence of this effect, the blades are rotating without any external load at the first 30 s to make sure the system reaches a stable status, and then the wind and wave loads are applied. Again, the results of the first 10 s after the application of the external loads are not analysed. All the results and discussions in this section are based on the numerical results within the time period of t = 40-230 s.

Fig. 18 shows the bi-directional motions at the top of the tower without and with the bi-directional TMD when the wind turbine is in the operating condition. Be more specific, the displacement time histories at the top of the tower in the in-plane and out-of-plane directions without and with different control methods are shown in Fig. 19. It should be noted that no external excitation is acting in the in-plane direction of the tower, its in-plane responses are induced by the interaction between the tower and blades. Table 7 tabulates the standard deviations of the in-plane and out-of-plane displacements at the top of the tower and the corresponding reduction ratios. As shown, for the wind turbine without any control device, the standard deviations of the in-plane and out-of-plane displacements are 0.0089 m and 0.0405 m respectively. When the bi-directional TMD system is installed, these values reduce to 0.0074 m and 0.0312 m, respectively and the corresponding reduction ratios are 16.9% and 23.0%. When the uniaxial TMD is used, the standard deviations of the displacements decrease to 0.0064 m and 0.0310 m and the reduction ratios are 28.1% and 23.5%, respectively. Again, the bi-directional

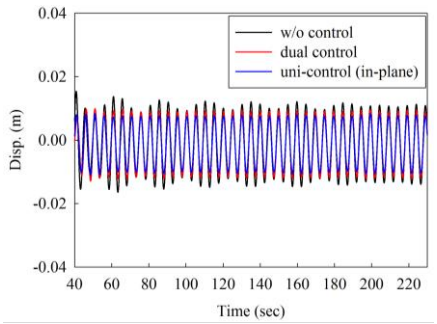

(a) In-plane

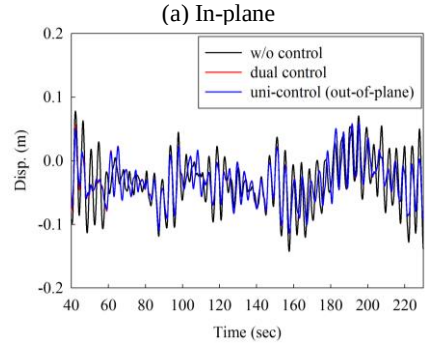

(b) Out-of-plane

Fig. 19 In-plane and out-of-plane displacements at the tower top under the operating condition

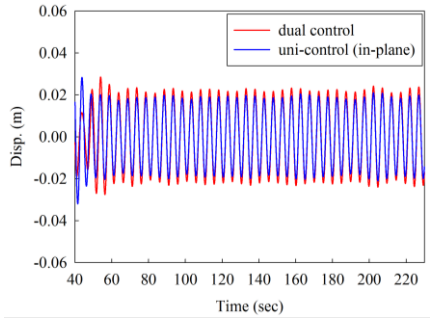

(a) In-plane TMD

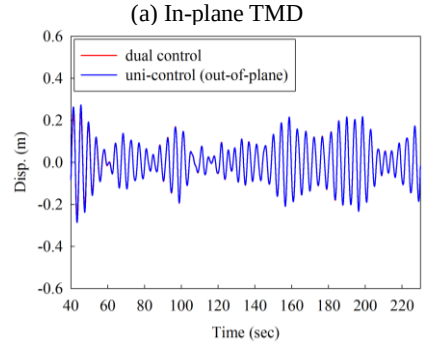

(b) Out-of-plane TMD

Fig. 20 Displacements of the in-plane and out-of-plane TMDs in the tower under the operating condition

Table 7 Standard deviations of the in-plane and out-of-plane displacements and the corresponding reduction ratios under the operating condition

Direction	Location	W/o control	Dual control		Uni-control	
		sd (m)	*sd* (m)	*R*	*sd* (m)	*R*
In-plane	Tower top	0.0089	0.0074	16.9%	0.0064	28.1%
	Tip of blade #2	0.1404	0.0885	37.0%	0.0666	52.6%
Out-of-plane	Tower top	0.0405	0.0312	23.0%	0.0310	23.5%
	Tip of blade #1	0.1646	0.1481	10.0%	0.1476	10.3%
	Tip of blade #2	0.1632	0.1481	9.3%	0.1475	9.6%
	Tip of blade #3	0.1567	0.1471	6.1%	0.1463	6.6%

TMD system moving in both the in-plane and out-of-plane directions slightly decreases the control effectiveness compared to the uniaxial TMD.

Fig. 20 shows the displacements of the in-plane and out-of-plane TMDs in the bi-directional and uniaxial control systems. As shown, the displacements of the in-plane TMD are quite small compared to the out-of-plane TMD because no external load is directly applied in the in-plane direction as discussed above. Due to the relatively small motions in the in-plane direction, the displacements of the out-of-plane TMD in the two control systems (i.e., the bi-directional and uniaxial control systems) are almost the same as shown in Fig. 20(b), which results in the similar control effectiveness in the out-of-plane direction as shown in Fig. 19(b) and Table 7.

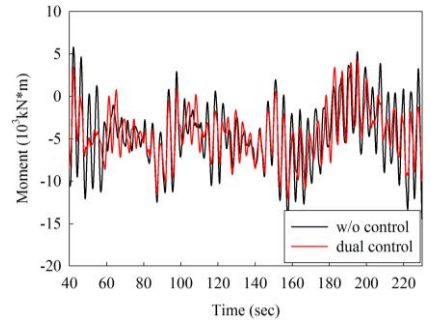

(a) In-plane

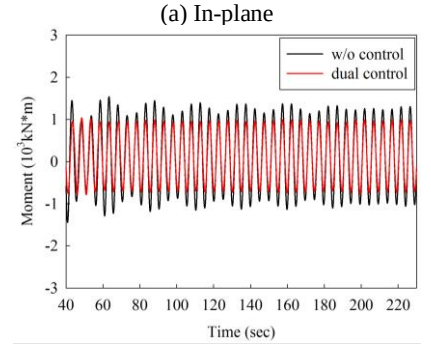

(b) Out-of-plane

Fig. 21 In-plane and out-of-plane bending moments at the tower bottom under the operating condition

Figs. 21 and 22 show the in-plane and out-of-plane bending moments and shear forces respectively at the tower bottom without and with the bi-directional TMD system

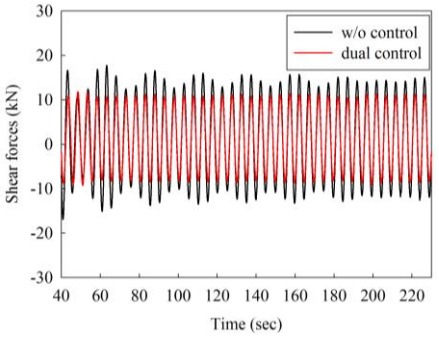

(a) In-plane

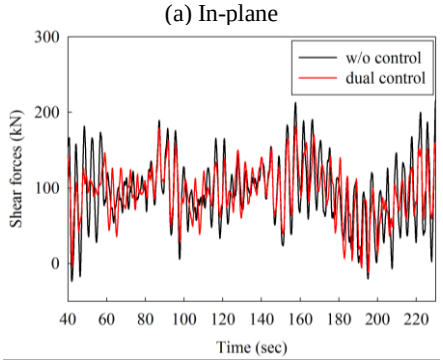

(b) Out-of-plane

Fig. 22 In-plane and out-of-plane shear forces at the tower bottom under the operating condition

Table 8 Standard deviations of the in-plane and out-of-plane bending moments and shear forces at the tower base and the corresponding reduction ratios under the operating condition

Inertial forces	Direction	W/o control	Dual control	
		sd	*sd*	*R*
Bending moment	In-plane	3780 kN·m	2901 kN·m	23.3%
	Out-of-plane	819 kN·m	598 kN·m	27.0%
Shear force	In-plane	9 kN	7 kN	22.2%
	Out-of-plane	44 kN	34 kN	22.7%

when the wind turbine is in the operating condition. The standard deviations of the bending moments and shear forces and the corresponding reduction ratios are summarized in Table 8. Again, as shown in the table, the bending moments and shear forces can be obviously mitigated by using the bi-directional TMD system and the reduction ratios are within the range of 22% to 27%.

As the in-plane and out-of-plane displacements of the three rotating blades have a similar trend, only the displacement responses at the tip of blade #2 are discussed herein. Fig. 23 shows the bi-directional motions at the tip of blade #2 without and with the bi-directional TMD when the wind turbine is in the operating condition, and Fig. 24 shows the displacement time histories at the tip of blade #2 in the in-plane and out-of-plane directions without and with different control systems. The standard deviations of the in-plane and out-of-plane displacements of the blades and the corresponding reduction ratios are also tabulated in Table 7.

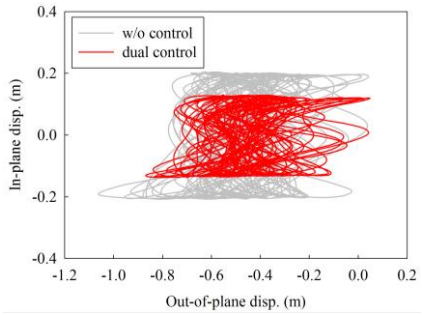

Fig. 23 Influence of bi-directional TMD system on the displacements of blade #2 under the operating condition

As shown, when the bi-directional system is installed, the standard deviation of the in-plane displacements at the tip of the blade decreases from 0.1404 m to 0.0885 m with a reduction ratio of 37.0%. For the uniaxial TMD system, the control effectiveness is more evident, and the reduction ratio reaches 52.6%. For the out-of-plane vibration, the control effectiveness is less evident compared to the in-plane motions, and the reduction ratios for the three blades vary from about 6% to 10%, which are at the same level as reported by Zuo *et al*. (2019). The effectiveness of the out-of-plane vibration control for the blades are different since the wind loads on the blades in the out-of-plane direction are influenced by the initial position as shown in Fig. 1(a), which results in the out-of-plane displacement responses of the three blades are not exactly the same.

6. Conclusions

In this paper, the bi-directional TMD system is proposed by adding another properly designed spring and dashpot to the perpendicular direction of the original TMD that is used to control the vibrations of wind turbines in one particular direction. With this minor change, the bi-directional TMD system can simultaneously mitigate the in-plane and out-of-plane vibrations of wind turbines subjected to the combined wind and sea wave loads. Moreover, a detailed 3D FE model of the wind turbine is developed in ABAQUS, and the control performance of the bi-directional TMD in two different operational conditions (i.e., parked and operating) of the wind turbine is investigated and compared with the uniaxial control system. The main conclusions are summarized as follows.

(1) When the wind turbine is in the parked condition, the in-plane and out-of-plane displacements of the tower are reduced by 37.3% and 40.0% by the bi-directional TMD, respectively. As for the in-plane and out-of-plane vibration mitigation of the blades, blade #1 achieves the largest reduction ratios, which are 12.8% and 20.1%, respectively.

(2) When the wind turbine is in the operating condition, the bi-directional TMD can reduce the in-plane and out-of-plane displacements of the tower by 16.9% and 23.0%, respectively. Moreover, the in-plane displacement of the blade is reduced by 37.0%, and the reduction ratios of the out-of-plane displacements of the three blades are within

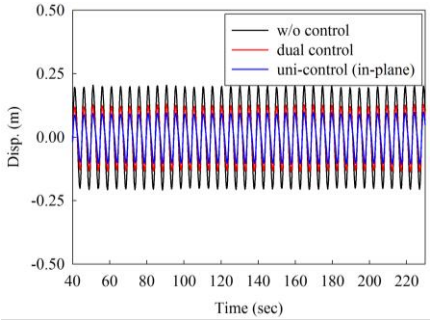

(a) In-plane

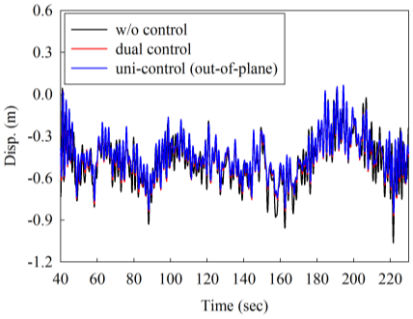

(b) Out-of-plane

Fig. 24 In-plane and out-of-plane displacements at the tip of blade #2 under the operating condition

the range of 6.1%-10.0%.

(3) The control effectiveness of the bi-directional TMD in the tower and blades is slightly smaller than that of the uniaxial control system at both the parked and operating conditions.

(4) The bending moments and shear forces at the tower bottom are substantially mitigated by the bi-directional TMD, and the reduction ratios are in the range of 22.2%-53.5% for the parked and operating conditions of the wind turbine. It indicates that the bi-directional control system is an efficient method to improve the reliability of wind turbines.

From a practical point of view, utilizing TMDs in mitigating the vibrations of offshore wind turbines is a cheap and robust solution, which have been widely used in engineering structures. Detailed design and installation are out-of-scope of the present study. Interested readers can refer to the sophisticated engineering practices of TMDs.

Acknowledgments

The authors would like to acknowledge the support from Australian Research Council Discovery Project DP190103279 for carrying out this research.

References

Arrigan, J., Huang, C., Staino, A., Basu, B. and Nagarajaiah, S. (2014), "A frequency tracking semi-active algorithm for control of edgewise vibrations in wind turbine blades", *Smart Struct. Syst., Int. J.*, **13**(2), 177-201. https://doi.org/10.12989/sss.2014.13.2.177.

Arrigan, J., Pakrashi, V., Basu, B. and Nagarajaiah, S. (2011), "Control of flapwise vibrations in wind turbine blades using semi-active tuned mass dampers", *Struct. Control Health Monit.*, **18**(8), 840-851. https://doi.org/10.1002/stc.404.

Basu, B., Zhang, Z. and Nielsen, S.R.K. (2016), "Damping of edgewise vibration in wind turbine blades by means of circular liquid dampers", *Wind Energy*, **19**(2), 213-226. https://doi.org/10.1002/we.1827.

Clough, R. and Penzien, J. (2003), *Dynamics of Structures*, Computer & Structures, Berkeley, CA, USA.

Colwell, S. and Basu, B. (2009), "Tuned liquid column dampers in offshore wind turbines for structural control", *Eng. Struct.*, **31**(2), 358-368. https://doi.org/10.1016/j.engstruct.2008.09.001.

Dinh, V.N., Basu, B. and Nagarajaiah, S. (2016), "Semi-active control of vibrations of spar type floating offshore wind turbines", *Smart Struct. Syst., Int. J.*, **18**(4), 683-705. http://dx.doi.org/10.12989/sss.2016.18.4.683.

DNV (2002), *Guidelines for Design of Wind Turbines*, Det Norske Veritas and Wind Energy Department, Risø National Laboratory, Copenhagen, Denmark.

DNV (2010), *DNV-RP-C205: Environmental Conditions and Environmental Loads*, Det Norske Veritas, Norway.

Fitzgerald, B. and Basu, B. (2014), "Cable connected active tuned mass dampers for control of in-plane vibrations of wind turbine blades", *J. Sound Vib.*, **333**(23), 5980-6004. https://doi.org/10.1016/j.jsv.2014.05.031.

Fitzgerald, B., Basu, B. and Nielsen, S.R.K. (2013), "Active tuned mass dampers for control of in-plane vibrations of wind turbine blades", *Struct. Control Health Monit.*, **20**(12), 1377-1396. https://doi.org/10.1002/stc.1524.

Ghassempour, M., Failla, G. and Arena, F. (2019), "Vibration mitigation in offshore wind turbines via tuned mass damper", *Eng. Struct.*, **183**, 610-636. https://doi.org/10.1016/j.engstruct.2018.12.092.

Global Wind Energy Council (2018), *Global Wind Report-Annual Market Update 2017*, GWEC.

Hansen, M.O.L. (2008), *Aerodynamics of Wind Turbines*, Earthscan, London, UK.

Hasselmann, K., Barnett, T., Bouws, E., Carlson, H., Cartwright, D., Enke, K., Ewing, J., Gienapp, H., Hasselmann, D. and Kruseman, P. (1973), "Measurements of wind-wave growth and swell decay", *Proceedings of the Joint North Sea Wave Project (JONSWAP)*, Hamburg, Germany, September.

Hemmati, A., Oterkus, E. and Khorasanchi, M. (2019), "Vibration suppression of offshore wind turbine foundations using tuned liquid column dampers and tuned mass dampers", *Ocean Eng.*, **172**, 286-295. https://doi.org/10.1016/j.oceaneng.2018.11.055.

Hu, Y., Wang, J., Chen, M.Z., Li, Z. and Sun, Y. (2018), "Load mitigation for a barge-type floating offshore wind turbine via inerter-based passive structural control", *Eng. Struct.*, **177**, 198-209. https://doi.org/10.1016/j.engstruct.2018.09.063.

Huang, G., Liao, H. and Li, M. (2013), "New formulation of Cholesky decomposition and applications in stochastic simulation", *Probabilistic Eng. Mech.*, **34**, 40-47. https://doi.org/10.1016/j.probengmech.2013.04.003.

Hussan, M., Rahman, M.S., Sharmin, F., Kim, D. and Do, J. (2018), "Multiple tuned mass damper for multi-mode vibration reduction of offshore wind turbine under seismic excitation", *Ocean Eng.*, **160**, 449-460. https://doi.org/10.1016/j.oceaneng.2018.04.041.

Jonkman, J., Butterfield, S., Musial, W. and Scott, G. (2009), "Definition of a 5-MW Reference Wind Turbine for Offshore System Development", Technical Report No. NREL/TP-500-38060, National Renewable Energy Laboratory, Golden, CO, USA.

Lackner, M.A. and Rotea, M.A. (2011), "Passive structural control of offshore wind turbines", *Wind Energy*, **14**(3), 373-388.

https://doi.org/10.1002/we.426.
Mensah, A.F. and Dueñas-Osorio, L. (2014), "Improved reliability of wind turbine towers with tuned liquid column dampers (TLCDs)", *Struct. Saf.*, **47**, 78-86. https://doi.org/10.1016/j.strusafe.2013.08.004.
Murtagh, P.J., Basu, B. and Broderick, B.M. (2005), "Along-wind response of a wind turbine tower with blade coupling subjected to rotationally sampled wind loading", *Eng. Struct.*, **27**(8), 1209-1219. https://doi.org/10.1016/j.engstruct.2005.03.004.
Murtagh, P.J., Ghosh, A., Basu, B. and Broderick, B.M. (2008), "Passive control of wind turbine vibrations including blade/tower interaction and rotationally sampled turbulence", *Wind Energy*, **11**(4), 305-317. https://doi.org/10.1002/we.249.
Staino, A., Basu, B. and Nielsen, S.R.K. (2012), "Actuator control of edgewise vibrations in wind turbine blades", *J. Sound Vib.*, **331**(6), 1233-1256. https://doi.org/10.1016/j.jsv.2011.11.003.
Stewart, G.M. and Lackner, M.A. (2014), "The impact of passive tuned mass dampers and wind–wave misalignment on offshore wind turbine loads", *Eng. Struct.*, **73**, 54-61. https://doi.org/10.1016/j.engstruct.2014.04.045.
Sun, C. and Jahangiri, V. (2018), "Bi-directional vibration control of offshore wind turbines using a 3D pendulum tuned mass damper", *Mech. Syst. Signal Process.*, **105**, 338-360. https://doi.org/10.1016/j.ymssp.2017.12.011.
Sun, C. and Jahangiri, V. (2019), "Fatigue damage mitigation of offshore wind turbines under real wind and wave conditions", *Eng. Struct.*, **178**, 472-483. https://doi.org/10.1016/j.engstruct.2018.10.053.
Sun, C., Jahangiri, V. and Sun, H. (2019), "Performance of a 3D pendulum tuned mass damper in offshore wind turbines under multiple hazards and system variations", *Smart Struct. Syst., Int. J.*, **24**(1), 53-65. http://dx.doi.org/10.12989/sss.2019.24.1.053.
Zhang, C., Li, L., and Ou, J. (2010), "Swinging motion control of suspended structures: Principles and applications", *Struct. Control Health Monit.*, **17**(5), 549-562. https://doi.org/10.1002/stc.331.
Zhang, C. (2014), "Control force characteristics of different control strategies for the wind-excited 76-story benchmark building structure", *Adv. Struct. Eng.*, **17**(4), 543-559. https://doi.org/10.1260/1369-4332.17.4.543.
Zhang, C. and Ou, J. (2015), "Modeling and dynamical performance of the electromagnetic mass driver system for structural vibration control", *Eng. Struct.*, **82**, 93-103. https://doi.org/10.1016/j.engstruct.2014.10.029.
Zhang, C. and Wang, H. (2019), "Robustness of the active rotary inertia driver system for structural swing vibration control subjected to multi-type hazard excitations", *Appl. Sci.*, **9**(20), 4391. https://doi.org/10.3390/app9204391.
Zhang, C. and Wang, H. (2020), "Swing vibration control of suspended structures using the active rotary inertia driver system: Theoretical modeling and experimental verification", *Struct. Control Health Monit.*, **27**(6), e2543. https://doi.org/10.1002/stc.2543.
Zhang, R., Zhao, Z. and Dai, K. (2019), "Seismic response mitigation of a wind turbine tower using a tuned parallel inerter mass system", *Eng. Struct.*, **180**, 29-39. https://doi.org/10.1016/j.engstruct.2018.11.020.
Zhang, Z., Li, J., Nielsen, S.R.K. and Basu, B. (2014), "Mitigation of edgewise vibrations in wind turbine blades by means of roller dampers", *J. Sound Vib.*, **333**(21), 5283-5298. https://doi.org/10.1016/j.jsv.2014.06.006.
Zhang, Z., Basu, B. and Nielsen, S.R.K. (2015a), "Tuned liquid column dampers for mitigation of edgewise vibrations in rotating wind turbine blades", *Struct. Control Health Monit.*, **22**(3), 500-517. https://doi.org/10.1002/stc.1689.
Zhang, Z., Nielsen, S.R.K., Basu, B. and Li, J. (2015b), "Nonlinear modeling of tuned liquid dampers (TLDs) in rotating wind turbine blades for damping edgewise vibrations", *J. Fluids Struct.*, **59**, 252-269. https://doi.org/10.1016/j.jfluidstructs.2015.09.006.
Zhang, Z., Staino, A., Basu, B. and Nielsen, S.R. (2016), "Performance evaluation of full-scale tuned liquid dampers (TLDs) for vibration control of large wind turbines using real-time hybrid testing", *Eng. Struct.*, **126**, 417-431. https://doi.org/10.1016/j.engstruct.2016.07.008.
Zhao, B., Gao, H., Wang, Z. and Lu, Z. (2018), "Shaking table test on vibration control effects of a monopile offshore wind turbine with a tuned mass damper", *Wind Energy*, **21**(12), 1309-1328. https://doi.org/10.1002/we.2256.
Zuo, H., Bi, K. and Hao, H. (2017), "Using multiple tuned mass dampers to control offshore wind turbine vibrations under multiple hazards", *Eng. Struct.*, **141**, 303-315. https://doi.org/10.1016/j.engstruct.2017.03.006.
Zuo, H., Bi, K. and Hao, H. (2018), "Dynamic analyses of operating offshore wind turbines including soil-structure interaction", *Eng. Struct.*, **157**, 42-62. https://doi.org/10.1016/j.engstruct.2017.12.001.
Zuo, H., Bi, K. and Hao, H. (2019), "Mitigation of tower and out-of-plane blade vibrations of offshore monopile wind turbines by using multiple tuned mass dampers", *Struct. Infrastruct. Eng.*, **15**(2), 269-284. https://doi.org/10.1080/15732479.2018.1550096.
Zuo, H., Bi, K., and Hao, H. (2020), "A state-of-the-art review on the vibration mitigation of wind turbines", *Renew. Sust. Energy Rev.*, **121**, 109710. https://doi.org/10.1016/j.rser.2020.109710.

BS